Journal of Cancer Research and Clinical Oncology (2019) 145:861–872
https://doi.org/10.1007/s00432-019-02845-y

ORIGINAL ARTICLE – CANCER RESEARCH

GLRX inhibition enhances the effects of geftinib in EGFR-TKI-resistant NSCLC cells through FoxM1 signaling pathway

Linlin Wang[1,3] · Jing Liu[2] · Jinguo Liu[1] · Xiaoyan Chen[1,3] · Meijia Chang[1,3] · Jing Li[1,3] · Jian Zhou[1,3] · Chunxue Bai[1,3] · Yuanlin Song[1,3]

Received: 28 May 2018 / Accepted: 11 January 2019 / Published online: 19 January 2019

Abstract

Purpose Non-small-cell lung cancer (NSCLC) is the most common form of lung cancer. Gefitinib is one of the most accepted therapies against NSCLC in those carrying *EGFR* mutations, but it is only effective in approximately 20% of patients with NSCLC. Thus, alternative therapeutic interventions are urgently needed to overcome gefitinib resistance. Glutaredoxin (GLRX) plays a key role in oxidative stress. However, whether GLRX inhibition could enhance gefitinib efficacy in the gefitinib-resistant NSCLC cells is unknown. In this study, we aimed to determine whether combined inhibition of GLRX could enhance growth-inhibitory effects of gefitinib in gefitinib-resistant NSCLC cells.

Methods Real-time PCR and western blotting were used to examine the mRNA and protein levels of GLRX in gefitinib-sensitive PC9 and HCC827 and -resistant human lung adenocarcinoma PC9R, HCC827R, and H1975 cells. Cell Counting Kit-8, flow cytometry, JC-1 staining, and reactive oxygen species (ROS) assays were used to evaluate cell proliferation, cell cycle progression, mitochondrial membrane potential, and ROS generation, respectively. Mouse tumor xenografts were used to assess the effect of GLRX in vivo.

Results We found that GLRX was upregulated in gefitinib-resistant PC9R, HCC827R, and H1975 cells. GLRX inhibition enhanced the effects of geftinib in gefitinib-resistant cell proliferation *in vitro* and in vivo and promoted apoptosis and cell cycle arrest via the EGFR/Forkhead Box M1 (FoxM1) signaling pathway, indicating that combined inhibition of GLRX could enhance growth-inhibitory effects of gefitinib in gefitinib-resistant NSCLC cells.

Conclusions Our results suggest that GLRX inhibition enhances the effects of geftinib in EGFR-TKI-resistant NSCLC cells. Thus, GLRX may represent a therapeutic target for increasing the efficiency of gefitinib treatment.

Keywords GLRX · Non-small-cell lung cancer · Gefitinib · Drug resistance · FoxM1

Introduction

Non-small-cell lung cancer (NSCLC) is the most common form of lung cancer and remains the leading cause of cancer-related deaths worldwide (Pao and Chmielecki 2010). Gefitinib, the first epidermal growth factor receptor (EGFR) tyrosine kinase inhibitor (TKI) to be identified, is one of the most accepted therapies against NSCLC in those carrying *EGFR* mutations (Nelson and Dolder 2006; Wakeling et al. 2002; Yewale et al. 2013). However, almost all NSCLC patients who initially respond well to EGFR-TKI therapy eventually develop acquired resistance (Rho et al. 2009). Thus, the development of effective therapeutic interventions to overcome gefitinib resistance is urgently needed.

EGFR is a member of the receptor tyrosine kinase family and promotes cell proliferation and survival. The

Linlin Wang, Jing Liu, Jinguo Liu contributed equally to this work.

✉ Jian Zhou
zhou.jian@fudan.edu.cn

✉ Chunxue Bai
bai.chunxue@zs-hospital.sh.cn

✉ Yuanlin Song
song.yuanlin@zs-hospital.sh.cn

[1] Department of Pulmonary Medicine, Zhongshan Hospital, Fudan University, 180 Fenglin Rd, Shanghai 200032, China

[2] Department of Pathology, The Affiliated Yantai Yuhuangding Hospital, Qingdao University, Yantai, China

[3] Shanghai Respiratory Research Institute, Shanghai, China

kinase-dependent activity of EGFR contributes to metastasis, poor prognosis, and resistance to chemotherapy in NSCLC (Nicholson et al. 2001). Clinically, the use of EGFR-TKIs, such as gefitinib, has not achieved maximum therapeutic efficacy (Kris 2002). Previous studies have shown that knockdown of EGFR leads to the inactivation of phosphorylated AKT (p-AKT) and cell apoptosis (Chen et al. 2012; Ewald et al. 2003; Feng et al. 2007; Nagy et al. 2003; Tan et al. 2015; Weihua et al. 2008), indicating that the kinase-independent activity of EGFR might also play an important role in gefitinib resistance.

The glutaredoxin subfamily belongs to the thiol-disulfide oxidoreductase family, and members contain conserved Cys-X-X-Cys domains in their active sites (Liu et al. 2015). There are two well-studied types of glutaredoxin: GLRX and GLRX2 (Holmgren 1976, 1979). GLRX is a cytosolic disulfide oxidoreductase, while GLRX2 localizes to the mitochondria and the nucleus (Gladyshev et al. 2001; Lundberg et al. 2001). GLRX specifically catalyzes protein deglutathionylation, which plays an important role in redox regulation in response to reactive oxygen species (ROS) (Gallogly et al. 2009), and the silencing of GLRX induces senescence in various cell types (Gallogly et al. 2010; Rodriguez-Rocha et al. 2012; Yang et al. 2018). GLRX is an antioxidant responsive element (ARE) dependent gene, which is the target of NRF2/KEAP1 pathway (Boddupalli et al. 2012). However, little is known regarding the regulation or function of GLRX expression in gefitinib-resistant cells.

FoxM1 is a member of the Forkhead box family of transcription factors. Previous studies have demonstrated that FoxM1 participates in gefitinib resistance by promoting cell proliferation and inhibiting apoptosis (Raychaudhuri and Park 2011; Sun et al. 2011). Furthermore, the inhibition of FoxM1 expression in resistant cells can partially restore sensitivity to gefitinib (Xu et al. 2012). FoxM1 also plays a critical role in the regulation of oxidative stress (Park et al. 2009). However, the relationship between GLRX and FoxM1 is unclear.

In this study, we aimed to determine the regulation and function of GLRX and its underlying mechanism in gefitinib resistance in NSCLC. Our results suggest that GLRX may play an important role in gefitinib resistance in NSCLC and that GLRX may represent a therapeutic target for overcoming resistance to gefitinib.

Materials and methods

Cells and cell culture

PC9 (exon 19 del, E746-A750), HCC827 (exon 19 del, E746-A750), and H1975 (intrinsically harbor EGFRL858R/T790M) human lung adenocarcinoma cells were purchased from the American Type Culture Collection (Manassas, VA, USA). To induce gefitinib resistance, PC9 and HCC827 cells were exposed to increasing concentrations of gefitinib. Gefitinib-sensitive PC9 and HCC827 and -resistant PC9R, HCC827R, and H1975 cells were cultured in Roswell Park Memorial Institute 1640 medium (RPMI-1640, Thermo Fisher Scientific, Waltham, MA, USA) supplemented with 10% heat-inactivated fetal bovine serum and 100 U/ml penicillin/streptomycin. Gefitinib resistance was maintained by adding 1 μM gefitinib (Selleckchem, Houston, TX, USA). Cells were grown as monolayers in a humidified atmosphere of 5% CO_2 at 37 °C. Bardoxolone methyl (Bardoxolone) or Sulforaphane were purchased from MCE (MedChem Express, New Jersey, USA).

Lentiviral construction and infection

Short hairpin (sh)RNA vectors targeting *GLRX* (shGLRX-1 and shGLRX-2), *EGFR* (shEGFR), and *FoxM1* (shFoxM1) were obtained from The RNAi Consortium (TRC). Lentiviral plasmids containing GV112-shGLRX-1, -shGLRX-2, -shEGFR, -shFoxM1, and -negative control shRNA were obtained from GeneChem (Shanghai, China). Lentivirus overexpressing human *EGFR* (PC9R-EGFR, GenBank accession number NM_005228) was purchased from GeneChem. Lentivirus overexpressing human *FoxM1* (PC9R-FoxM1, GenBank accession number NM_202002.2) was obtained from GeneCopoeia (Germantown, MD, USA). Lentiviral particles were produced by transfecting HEK293T cells with lentiviral plasmids. For viral infection, PC9R cells were plated in 6-well plates, grown to 50–70% confluence, and incubated with medium containing virus and 4 μg/ml polybrene at a multiplicity of infection (MOI) of 10. The infected cells were then incubated with various concentrations of gefitinib 24 h after infection.

Small interfering RNA (siRNA) transfection

Transfections were performed using the Santa Cruz Biotechnology transfection reagent according to the manufacturer's protocol. The following sequences were used for siRNA transfections: siNRF2-1 (sense, CCCGUUUGUAGAUGACAAUTT, antisense, AUUGUCAUCUACAAACGGGTT), siNRF2-2 (sense, GCCCAUUGAUGUUUCUGAUTT, antisense, AUCAGAAACAUCAAUGGGCTT), and negative control (siCtrl) (sense, UUCUCCGAACGUGUCACGUTT, antisense, ACGUGACACGUUCGGAGAATT) was synthesized by GenePharma (Shanghai, China).

Cell proliferation and viability assay

Cell Counting Kit-8 (CCK-8; Dojindo Laboratories, Kumamoto, Japan) was used to assess cell proliferation. Briefly,

cells were plated in 96-well plates at approximately 1000 cells per well with 200 µl of culture medium. After 24 h, 10 µl of CCK-8 solution was applied to each well, and the plates were incubated for 1 h at 37 °C. Finally, the light absorbance values at 450 nm were determined using a microplate reader (Multiskan, Thermo Fisher Scientific) with a reference wavelength of 650 nm. All experiments were conducted at least in triplicate.

EdU incorporation assay

Cells were incubated with 10 µM EdU (5-ethynyl-2′-deoxyuridine, Thermo Fisher Scientific) for 4 h and were then fixed in 3.7% formaldehyde in PBS for 15 min at room temperature. EdU was detected to determine EdU incorporation according to the manufacturer's recommendations. Confocal imaging was performed on a Nikon A1R confocal laser scanning microscope system (Nikon Corp., Tokyo, Japan). PC9R cells positive for EdU incorporation and positive for Hoechst 33,342 staining were counted using ImageJ (v. 1.42, National Institutes of Health, Bethesda, MD, USA) and were used to calculate the percentage of EdU-positive cells.

Detecting apoptosis by flow cytometry

An annexin V-allophycocyanin (APC)/ 4′,6-diamidino-2-phenylindole (DAPI) double staining kit (Thermo Fisher Scientific) was used to analyze cellular apoptosis. Infected PC9R cells were seeded in 6-well plates (5×10^5 cells/well) and treated with 1 µM gefitinib. Cells were then digested with trypsin (Gibco® trypsin–EDTA, Thermo Fisher Scientific), washed with PBS three times, suspended in 500 µl of binding buffer, and then incubated with 5 µl of FITC-conjugated annexin V and 3 µl of PI for 15 min at room temperature in the dark. The stained cells were detected using the BD FACS Aria II flow cytometer (BD Biosciences, Hercules, CA, USA).

Cell cycle analysis

Infected PC9R cells were seeded in 6-well plates (5×10^5 cells/well) and treated with 1 µM gefitinib. Treated cells were then collected, washed with PBS, and fixed in 70% ethanol for 24 h at 4 °C. Fixed cells were stained with PI in the dark for 30 min at room temperature. Finally, cell cycle distributions were analyzed by flow cytometry on a BD FACS Aria II flow cytometer (BD Biosciences).

Mitochondrial membrane potential measurement

The MitoProbe™ JC-1 assay kit (Thermo Fisher Scientific) was used to detect changes in the mitochondrial membrane potential. The assay was performed according to the manufacturer's instructions, and the results were obtained by BD FACS Aria II flow cytometer.

Measurement of ROS levels

Reactive oxygen species (ROS) were detected using the CellROX Orange probe (Invitrogen). Infected PC9R cells were seeded in 6-well plates (5×105 cells/well) and treated with 1 µM gefitinib. Cells were digested with trypsin–EDTA, incubated with 5 µM CellROX Orange reagent at 37 °C for 30 min, washed twice with PBS, and analyzed by flow cytometry to quantify ROS.

Quantitative RT-PCR

Total RNA was extracted using the TRIzol reagent (Thermo Fisher Scientific). RNA (1%) was reverse-transcribed into cDNA using reverse transcriptase (Toyobo, Osaka, Japan), and 20 ng cDNA was used as the template for RT-PCR. The amplification cycling parameters (40 cycles) were set as follows: 15 s at 95 °C, 15 s at 60 °C, and 45 s at 72 °C. The primer sequences included the following: GLRX sense 5′-GGGAAGGTGGTTGTGTTCAT-3′, anti-sense 5′-TAG TGTGGTTGGTGGCTGTG-3′; FoxM1 sense 5′-AAG AACTCCATCCGCCACAAC-3′, anti-sense 5′-GCTTAA ACACCTGGTCCAATGTC-3′; NRF2 sense 5′-GTCACA TCGAGAGCCCAGTC-3′, anti-sense 5′-AGCTCCTCC CAAACTTGCTC-3′; β-actin sense 5′-CTGGCACCCAGC ACAATG-3′, anti-sense 5′-CCGATCCACACGGAGTAC TTG-3′. Gene expression levels were normalized to those of β-actin and calculated using the $2^{-\Delta\Delta CT}$ method. Each RT-PCR assay was performed at least three separate times in triplicate.

Western blotting assay

Total proteins from PC9, PC9R, HCC827, HCC827R, and H1975 cells were extracted using a RIPA kit (Beyotime Biotechnology, Jiangsu, China). They were separated on polyacrylamide gels and transferred to PVDF membranes. The membranes were incubated with anti-GLRX (Abcam, Cambridge, MA, USA), anti-EGFR [Cell Signaling Technology (CST), Danvers, MA, USA], anti-FoxM1 (Sigma, St. Louis, MO, USA), anti-p-AKT (CST), anti-AKT (CST), anti-p-ERK (Phospho-p44/42 MAPK, Thr202/Tyr204, CST), anti-ERK (ERK1/2, Proteintech, Rosemont, IL, USA), anti-cleaved caspase-3 (Asp175, CST), anti-cleaved PARP (Asp214, CST), and anti-actin (CST) antibodies at 4 °C overnight and were then incubated with horseradish peroxidase-conjugated goat anti-rabbit or anti-mouse immunoglobulin G at room temperature for 1 h. Proteins were visualized using Pierce ECL Western Blotting substrate and

autoradiography. Blots were analyzed using Quantity One 4.6.

cDNA array screening

Total RNA was extracted using RNeasy Plus Mini Kit (Qiagen, Valencia, CA, USA) from PC9R cells expressing shGLRX-1 or negative control shRNA, reverse transcribed, and amplified using OneArray Plus RNA Amplification Kit (Phalanx Biotech Group, Taiwan). Cy5-labeled amplicons were hybridized to Human Whole Genome OneArray (Phalanx Biotech Group), imaged on a G2505C Agilent Microarray Scanner (Agilent Technologies, Santa Clara, CA, USA), and analyzed in Resolver (Rosetta Biosoftware, Seattle, WA, USA).

Tumorigenicity evaluation

All animal experiments were approved by the Institutional Animal Care and Use Committee of Zhongshan Hospital, Fudan University, Shanghai, China. Four- to 6-week-old male BALB/c nude mice were obtained from the Shanghai Experimental Animal Center of the Chinese Academy of Sciences (Shanghai, China). PC9R cells infected with shGLRX-1 or negative control shRNA were subcutaneously injected into the right flanks of nude mice. The tumor volume was monitored and calculated according to the following formula: volume = Length × Width^2/2. After one month, tumors were dissected out and weighed. Ki67 immunohistochemical staining was used to identify proliferating cells in paraffin sections of the xenograft tumors. Ki67-positive cells were quantified in randomly selected fields from each tissue section using ImageJ.

Statistical analysis

Data are expressed as the means ± SD of at least three independent experiments. A one-way analysis of variance (ANOVA) followed by Bonferroni's multiple comparison test was applied to compare differences among multiple groups. Student's *t* test was applied to compare differences between two groups. A P value of < 0.05 was considered statistically significant.

Results

GLRX is upregulated in gefitinib-resistant cells and mediates gefitinib resistance

We established a gefitinib-resistant cell line, PC9R, by continuously exposing PC9 cells to increasing concentrations of gefitinib. We used quantitative reverse transcription (qRT)-PCR and western blotting analyses to investigate the mRNA and protein expression levels of GLRX. We found that GLRX was significantly upregulated in PC9R cells compared to levels in PC9 cells (Fig. 1a, b). The protein level of GLRX in gefitinib-sensitive PC9 cells was reduced after treatment with 0.1 μM gefitinib (Fig. 1c); however, the protein level of GLRX in gefitinib-resistant PC9R cells was not reduced after treatment with 0.1 μM gefitinib (Fig. 1d). Furthermore, we found that compared to gefitinib-sensitive PC9 and HCC827 cells, the protein level of GLRX was upregulated in gefitinib-resistant HCC827R and H1975 cells (Fig. 1e). These results indicated that GLRX may play an important role in gefitinib resistance. To confirm this, PC9R cells were infected with either shRNA targeting *GLRX* or negative control shRNA to silence GLRX expression. Subsequent qRT-PCR and western blotting analyses showed that shGLRX-1 and -2, two shRNA sequences targeting the *GLRX* transcript, significantly inhibited GLRX expression (Fig. 1f, g). Morphological examination indicated that knockdown of GLRX led to reduced cell numbers after treatment of gefitinib-resistant cells with 1 μM gefitinib for 96 h (Fig. 1h). To verify this, CCK-8 assays revealed that infection of PC9R cells with either shGLRX-1 or -2 enhanced the gefitinib-mediated cell proliferation inhibition, especially at 10.0 μM gefitinib, increasing the percentage of cell proliferation inhibition from 30 to 53 or 56%, respectively (Fig. 1i, j).

Knockdown of GLRX inhibits gefitinib-resistant cell proliferation in vitro and vivo

To investigate the function of GLRX in gefitinib-resistant cell proliferation, EdU staining was performed (Fig. 2a). GLRX silencing suppressed the proliferation of gefitinib-resistant PC9R cells in the presence of 1 μM gefitinib (Fig. 2b), implying that GLRX promotes proliferation in gefitinib-resistant cells.

To determine whether GLRX knockdown reduces lung tumor growth in vivo, PC9R cells infected with shGLRX-1 were injected into nude mice. The volumes of tumors derived from GLRX-silenced cells were significantly reduced compared to those of tumors from control cells after about one month (Fig. 3a). A similar trend in tumor weight was observed after about one month (Fig. 3b). In consistent with this, the percentage of proliferating Ki67-positive cells was lower in GLRX-deficient tumors than in control xenografts (Fig. 3c, d). The western blotting analyses confirmed that the protein level of GLRX is reduced in tissue from GLRX-deficient tumors in comparison to that from control xenografts (Fig. 3e).

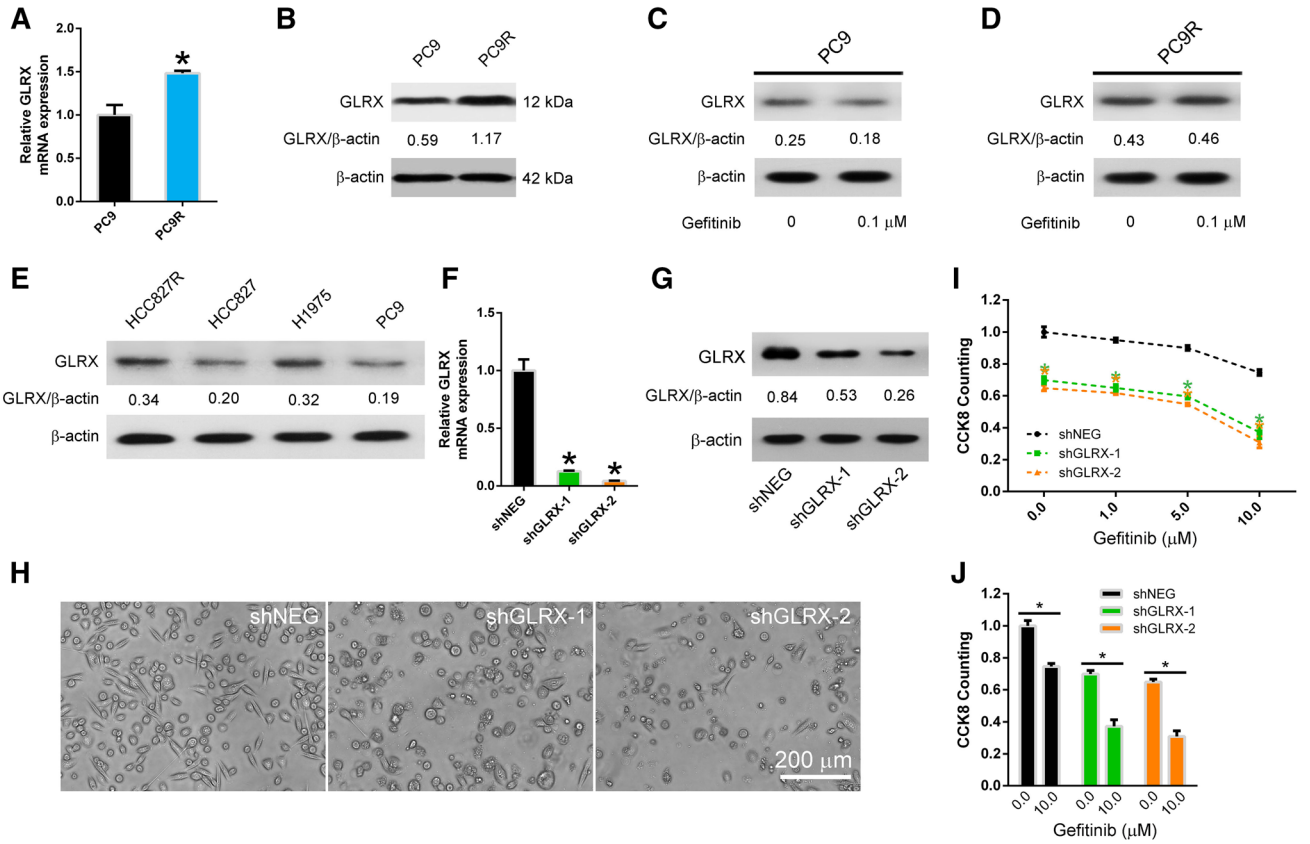

Fig. 1 GLRX is upregulated in gefitinib-resistant cells and confers gefitinib resistance. **a, b** GLRX expression in gefitinib-sensitive PC9 and gefitinib-resistant PC9R cells, as assessed by qRT-PCR and western blotting. **c, d** Western blotting of GLRX expression in PC9 and PC9R cells treated with 0.1 μM gefitinib for 24 h. **e** Western blotting of GLRX expression in gefitinib-sensitive PC9 and HCC827 and gefitinib-resistant HCC827R and H1975 cells. **f, g** qRT-PCR and western blotting of GLRX expression in PC9R cells transfected with shGLRX or negative control shRNA (shNEG). **h** Morphology of PC9R cells infected with shGLRX or shNEG and cultured in 1 μM gefitinib. **i, j** Viability of PC9R cells infected with shGLRX or shNEG and treated with different concentrations of gefitinib, as determined by CCK-8 assay. Data are representative of at least three similar experiments. $^*P < 0.05$ vs. negative control

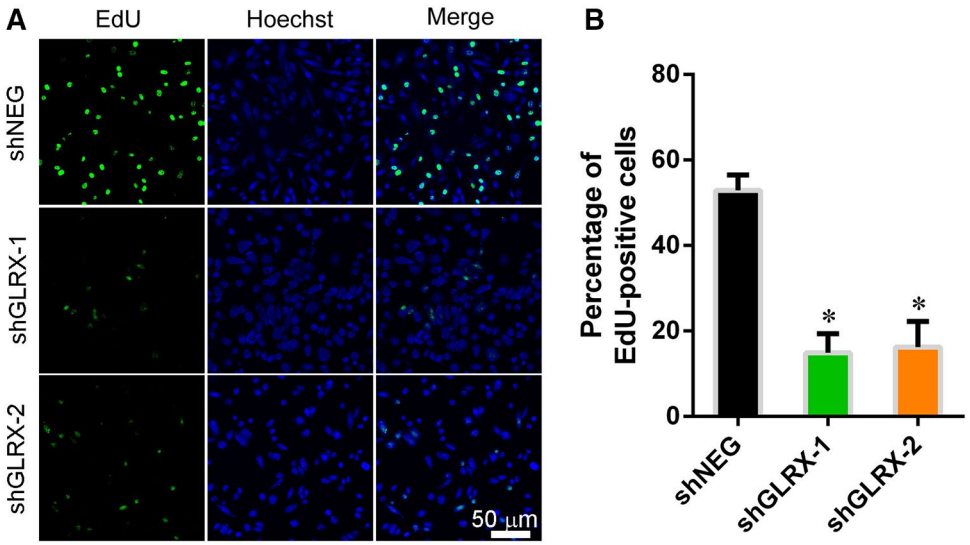

Fig. 2 Knockdown of GLRX inhibits proliferation of gefitinib-resistant cells. **a** PC9R cells infected with GLRX shRNA or negative control (shNEG) were treated with 1 μM gefitinib and then stained with EdU and Hoechst 33342. **b** EdU-stained cells were more abundant in control cells than in GLRX-depleted cells. Data are representative of at least three similar experiments. $^*P < 0.05$ vs. negative control

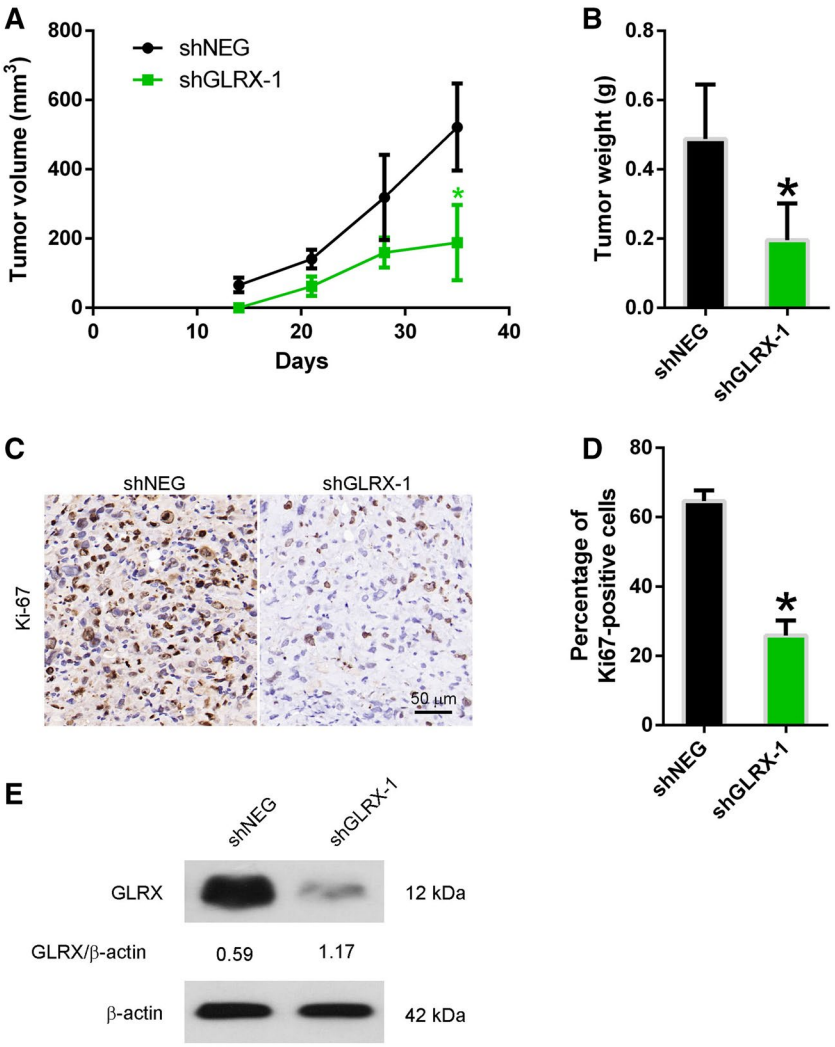

Fig. 3 GLRX knockdown suppresses tumor cell proliferation in vivo. **a** Tumor volume was measured once a week about 2 weeks after injection of PC9R cells infected with shGLRX-1 or negative control (shNEG). **b** Tumor weight. **c** Representative Ki67 expression in xenograft tumors. **d** Ki67-positive cells were quantified in randomly selected fields, $n=4$ mice per group. $^*P<0.05$ vs. negative control. **e** Western blotting of GLRX expression in tumor tissue from GLRX-deficient tumors and control xenografts

GLRX silencing promotes apoptosis and cell cycle arrest in gefitinib-resistant cells through caspase activation and mitochondrial dysfunction

To further confirm the effect of GLRX on gefitinib resistance, we analyzed rates of apoptosis using annexin V-APC/DAPI double staining and flow cytometry. In the presence of 1 μM gefitinib, the apoptotic rate of GLRX-silenced PC9R cells was higher than that of control cells (Fig. 4a, b). Moreover, the proportions of cells in S phase were reduced upon GLRX silencing, while cells in G2/M phase increased, indicating cell cycle arrest (Fig. 4c, d). We also assessed mitochondrial integrity by staining cells with JC-1 and measuring the mitochondrial membrane potential. The JC-1 monomer ratio of GLRX-silenced PC9R cells was higher than that of control cells in the presence of 1 μM gefitinib (Fig. 4e, f).

Since GLRX plays a key role in oxidative stress (Gallogly et al. 2009), we next investigated the role of GLRX in ROS generation. We found that ROS generation of GLRX-silenced PC9R cells was higher than that in control cells in the presence of 1 μM gefitinib (Fig. 4g, h). Moreover, cleaved caspase-3 and cleaved poly-ADP-ribose polymerase (PARP), two apoptotic proteins, were upregulated in GLRX-depleted cells compared with levels in control cells (Fig. 4i).

GLRX regulates gefitinib-resistance via EGFR/ FoxM1 signaling pathway

To evaluate the molecular mechanism underlying GLRX-mediated gefitinib resistance, we used a human whole-genome cDNA array and investigated changes in GLRX downstream signaling pathways upon GLRX silencing (Fig. 5a). Western blotting confirmed that EGFR and FoxM1 levels were markedly reduced in cells infected with shGLRX-1 or -2 compared to levels in cells infected with negative control shRNA (Fig. 5b).

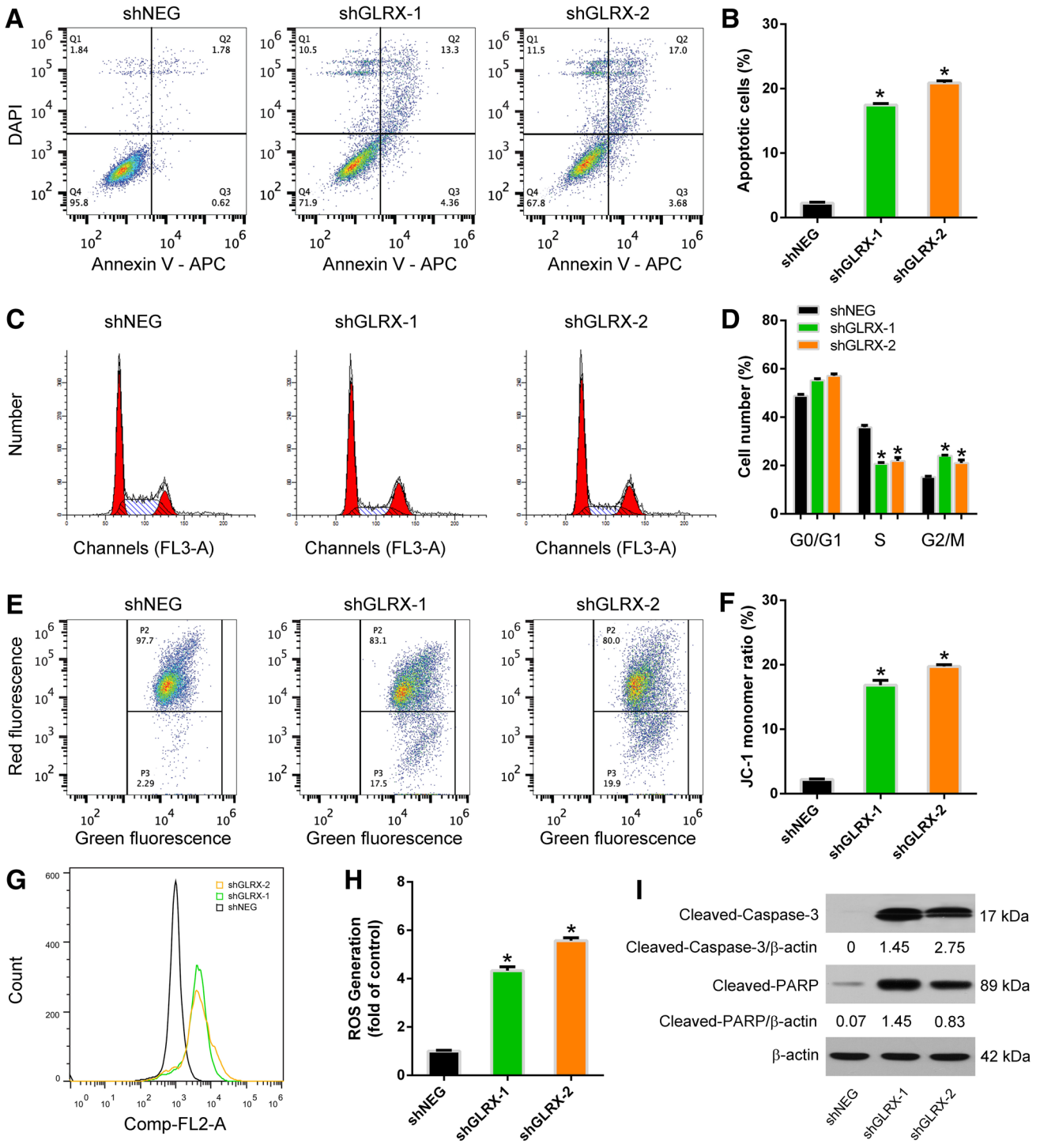

Fig. 4 GLRX silencing promotes G2/M arrest and apoptosis in gefitinib-resistant cells through caspase activation and mitochondrial damage. **a**–**b** PC9R cells infected with GLRX shRNA or negative control (shNEG) were treated with 1 μM gefitinib, stained with annexin V-APC/DAPI, and then analyzed by flow cytometry. GLRX silencing increased apoptosis. **c, d** PC9R cells expressing GLRX shRNA or shNEG were treated with 1 μM gefitinib, and cell cycle distribution was assessed by flow cytometry. **e, f** Representative histograms of JC-1 staining as measured by flow cytometry. GLRX silencing increased the proportion of JC-1 monomers in GLRX-depleted cells following incubation with 1 μM gefitinib. **g, h** Detection of ROS by flow cytometry. GLRX silencing increased ROS generation in PC9R cells relative to levels in shNEG-infected cells following incubation with 1 μM gefitinib. **I**) Western blotting of cleaved caspase-3 and cleaved PARP in PC9R cells infected with shGLRX or shNEG. Data are representative of three similar experiments. $^*P < 0.05$ vs. negative control

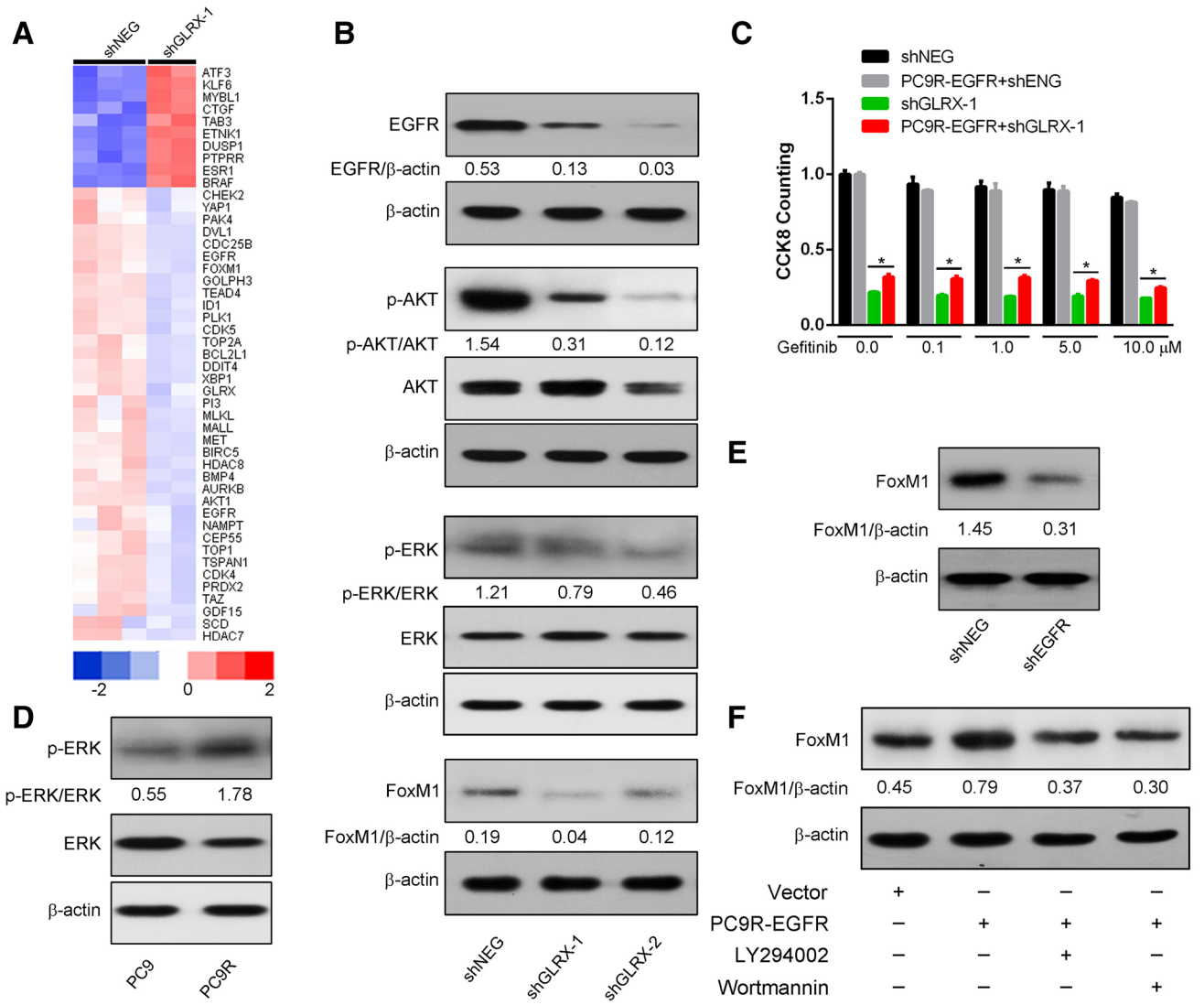

Fig. 5 Knockdown of GLRX suppresses EGFR/p-AKT/FoxM1 signaling pathway. **a** Human whole-genome cDNA array screening. **b** Protein levels of EGFR, p-AKT, AKT, p-ERK, ERK, and FoxM1 were determined by western blotting in PC9R cells infected with shGLRX or negative control shRNA (shNEG). **c** Proliferation of PC9R cells co-infected with EGFR (PC9R-EGFR) and shGLRX or shNEG, as determined by CCK-8 assay. **d** Protein levels of p-ERK and ERK were determined by western blotting in PC9 and PC9R cells. **e** Protein levels of FoxM1 were determined by western blotting in PC9R cells infected with shEGFR or shNEG. **f** Protein levels of FoxM1 were determined by western blotting in PC9R cells infected with EGFR (PC9R-EGFR) or shNEG in the presence or absence of 20 μm LY294002 and 10 μm wortmannin

Given that EGFR signaling plays a crucial role in NSCLC progression (Chen et al. 2012; Tan et al. 2015; Yamanaka et al. 2008; Zhang et al. 2018), we speculated that GLRX may confer gefitinib resistance through EGFR signaling. To evaluate this possibility, we performed rescue assays in PC9R cells. Using the CCK-8 assay, we found that overexpression of EGFR in PC9R cells partially rescued cell viability in the presence of gefitinib. These results suggest that overexpression of EGFR partially reversed the cell proliferation inhibition induced by GLRX depletion (Fig. 5c).

The PI3K/AKT (Chen et al. 2012; Ewald et al. 2003; Feng et al. 2007; Nagy et al. 2003; Tan et al. 2015; Weihua et al. 2008) and ERK (Ercan et al. 2012) pathways are the main downstream effectors of EGFR; thus, we examined levels of p-AKT/AKT and p-ERK/ERK in GLRX-silenced cells. Western blotting showed that p-AKT/AKT and p-ERK/ERK were inhibited in cells infected with shGLRX-1 or -2 compared to levels in cells infected with negative control shRNA (Fig. 5b), indicating that the p-AKT/AKT and p-ERK/ERK signaling pathways may play an important role in GLRX-mediated gefitinib resistance. Western blotting confirmed

that p-ERK/ERK was upregulated in gefitinib-sensitive PC9 compared to gefitinib-resistant PC9R cells (Fig. 5d).

FoxM1 plays an important role in gefitinib resistance (Xu et al. 2012); however, the relationship between EGFR and FoxM1 remains unclear. Next, we investigated FoxM1 protein expression in PC9R cells after silencing EGFR, and we observed that FoxM1 protein level was markedly downregulated in cells infected with shEGFR compared to level in cells infected with negative control shRNA (Fig. 5e). Consistent with this, EGFR overexpression had the opposite effect (Fig. 5f). Furthermore, treatment with the PI3K/AKT inhibitors LY294002 (20 μm and wortmannin (10 μm led to reduced level of FoxM1 protein in EGFR-overexpressing PC9R cells (Fig. 5f), indicating that EGFR may regulate FoxM1 via the PI3K/AKT pathway.

To confirm the function of FoxM1 in GLRX-mediated gefitinib resistance, PC9R cells were infected with either *FoxM1*-targeted or negative control shRNA to silence FoxM1 expression. qRT-PCR showed that shFoxM1 inhibited *FoxM1* expression (Fig. 6a). We first confirmed that knockdown of FoxM1 reduced the viability of gefitinib-resistant PC9R cells by treating silenced and control cells with various gefitinib concentrations (ranging from 0.1 to 10.0 μM) (Fig. 6b). To further confirm the role of FoxM1 in gefitinib resistance, we analyzed rates of apoptosis using annexin V-APC/DAPI double staining and flow cytometry. Upon treatment with 1 μM gefitinib, the apoptotic rate of FoxM1-silenced PC9R cells was higher than that of control cells (Fig. 6c). Moreover, the proportions of cells in G0/G1 and S phase were reduced upon FoxM1 silencing, while

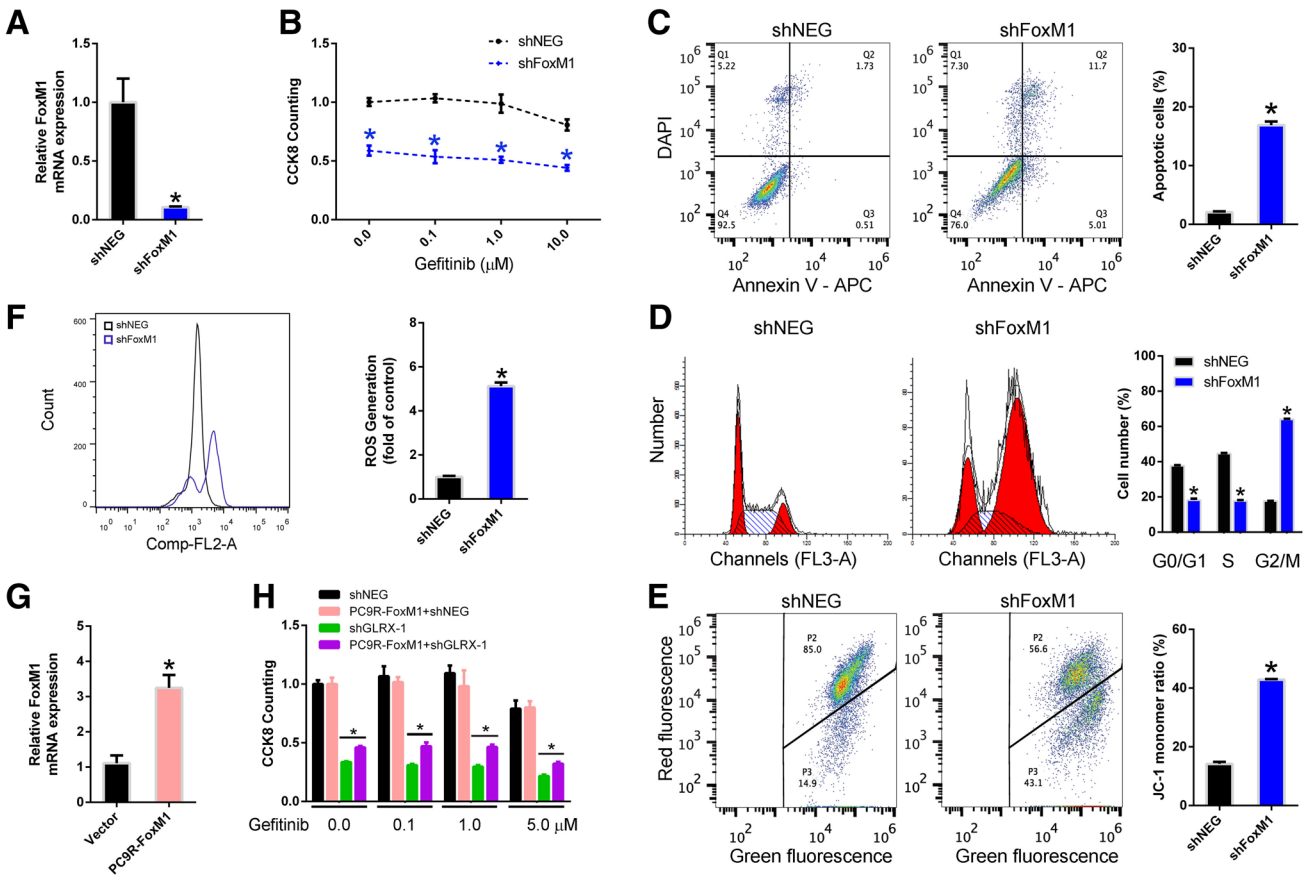

Fig. 6 FoxM1 confers gefitinib resistance. **a** qRT-PCR of *FoxM1* expression in PC9R cells infected with shFoxM1 or negative control shRNA (shNEG). **b** Viability of PC9R cells infected with shFoxM1 or shNEG and treated with different concentrations of gefitinib, as determined by CCK-8 assay. Data are representative of at least three similar experiments. $*P<0.05$ vs. negative control. **c** PC9R cells expressing FoxM1 shRNA or shNEG were treated with 1 μM gefitinib, stained with annexin V-APC/DAPI, and then analyzed by flow cytometry. GLRX silencing increased apoptosis. **d** PC9R cells expressing FoxM1 shRNA or shNEG were treated with 1 μM gefitinib, and cell cycle distribution was assessed by flow cytometry. **e** Representative histograms of JC-1 staining as measured by flow cytometry. FoxM1 silencing increased the proportion of JC-1 monomers in FoxM1-depleted cells following incubation with 1 μM gefitinib. **f** Detection of ROS levels by flow cytometry. FoxM1 silencing increased ROS generation in PC9R cells relative to those in cells infected with shNEG following incubation with 1 μM gefitinib. **g** qRT-PCR of *FoxM1* expression in PC9R cells infected with PC9R-FoxM1 or shNEG. **h** Proliferation of PC9R cells co-infected with PC9R-FoxM1 and shGLRX or shNEG, as determined by CCK-8 assay

those in G2/M phase increased (Fig. 6d). We also observed that the JC-1 monomer ratio and levels of ROS generation in FoxM1-silenced PC9R cells were higher than those in control cells in the presence of 1 μM gefitinib (Fig. 6e, f).

To further confirm that GLRX mediates gefitinib resistance through FoxM1 signaling, PC9R cells were infected with PC9R-FoxM1, a lentivirus conferring overexpression of human FoxM1. qRT-PCR showed that PC9R-FoxM1 infection increased the expression of *FoxM1* (Fig. 6g). Next, we performed a rescue assay in PC9R cells and found that overexpression of FoxM1 in the GLRX-depleted PC9R cells rescued cell viability in the presence of gefitinib. These results suggest that the overexpression of FoxM1 partially reverses the cell proliferation inhibition induced by GLRX depletion (Fig. 6h).

NRF2 regulates GLRX in gefitinib resistant PC9R cells

GLRX is an ARE dependent gene, which is the target of NRF2/KEAP1 pathway (Boddupalli et al. 2012). To conform this, we applied two distinct pools of siRNA to knockdown NRF2 in PC9R cells. qRT-PCR showed that both siNRF2-1 and siNRF2-2 significantly reduced the mRNA level of NRF2 in gefitinib resistant PC9R cells compared to the negative control siRNA (Fig. 7a). NRF2 siRNA knockdown resulted in the down-regulation GLRX (Fig. 7a). Furthermore, treatment of PC9R cells with 0.5 μM Bardoxolone or 10 μm Sulforaphane, activators of NRF2, for 24 h significantly increased the mRNA level of GLRX (Fig. 7b).

Discussion

NSCLC is the leading cause of cancer-related deaths worldwide. Gefitinib, an EGFR inhibitor, blocks downstream signaling pathways by competitively binding to the EGFR tyrosine kinase domain, but it is only effective in approximately 20% of patients with NSCLC (Chen et al. 2012; Mollbrink et al. 2014; Tan et al. 2015; Yamanaka et al. 2008). GLRX is a small protein catalyzing glutathione-dependent disulfide oxidoreduction reactions in a coupled system with NADPH, GSH, and glutathione reductase. It is necessary for the reduction of disulfides and is capable of catalyzing both deglutathionylation and the reverse of *S*-glutathionylation (Gallogly et al. 2009). Previous studies have found that the expression of GLRX correlates with the prognosis and metastasis of hepatocellular carcinoma (Mollbrink et al. 2014). However, data on the expression and function of GLRX in NSCLC gefitinib resistance are scarce. In this study, we showed that GLRX is upregulated in gefitinib-resistant PC9R cells. Additionally, to determine whether GLRX has the ability to confer resistance to NSCLC cells exposed to gefitinib, we knocked down GLRX expression in gefitinib-resistant cells. The results showed that when GLRX was inhibited, proliferation was suppressed and apoptosis and cell cycle arrest were promoted in gefitinib-resistant cells. Our results are consistent with those of previous studies demonstrating that knockdown of GLRX reduces proliferation in various cell types by increasing ROS (Yang et al. 2018).

To further determine the molecular mechanism by which GLRX contributes to gefitinib resistance in PC9R cells, the expression levels of EGFR and FoxM1 were assessed. We found that EGFR and FoxM1 levels were markedly downregulated in gefitinib-resistant cells after GLRX inhibition and that overexpression of EGFR or FoxM1 partially reversed the apoptosis induced by GLRX depletion. FoxM1 is a member of the Forkhead box family of transcription factors and regulates molecular events related to cell proliferation and cell cycle progression. It is overexpressed in many types of solid tumors and mediates the inherent resistance of NSCLC cells to EGFR-TKIs, including gefitinib (Elzagallaai et al. 2011; Raychaudhuri and Park 2011; Sun et al. 2011; Xu et al. 2012; Yu et al. 2011). Due to these properties, FoxM1 is currently attracting substantial interest as a potential target in cancer diagnosis and therapy. EGFR is a member of the receptor tyrosine kinase family that promotes cell proliferation and survival (Yewale et al. 2013). However, the

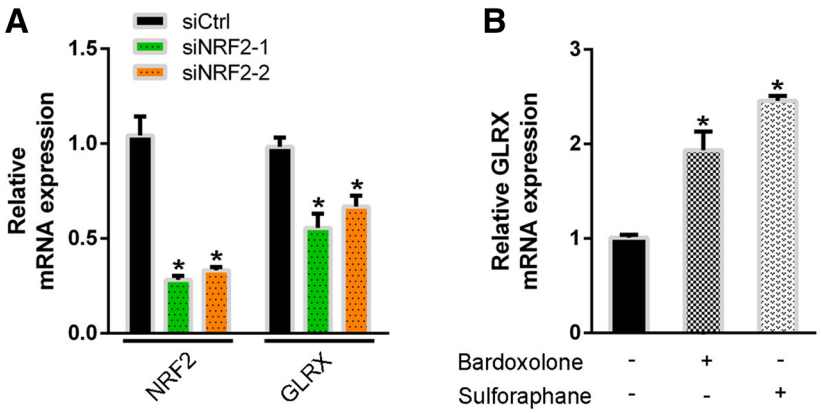

Fig. 7 NRF2 regulates GLRX in gefitinib resistant PC9R cells. **a** qRT-PCR of *NRF2* and *GLRX* expression in PC9R cells transfected with siNRF2 or negative control siRNA (siCtrl). $^*P < 0.05$ vs. negative control. **b** qRT-PCR of *GLRX* expression in PC9R cells treated with 0.5 μm Bardoxolone or 10 μm Sulforaphane for 24 h. $^*P < 0.05$ vs. untreated control PC9R cells

relationship between EGFR and FoxM1 in gefitinib-resistant cells was previously unclear. In this study, we found that FoxM1 was markedly reduced when EGFR was silenced, implying that GLRX may regulate gefitinib resistance via the EGFR/FoxM1 signaling pathway.

The PI3K/AKT pathway is one of the downstream signaling pathways of EGFR and is involved in regulating multiple cellular functions, including growth, differentiation, proliferation, survival, motility, invasion, and intracellular trafficking (Vara et al. 2004). Regulation of this pathway is associated with resistance to EGFR-TKI therapy and reduced survival in NSCLC patients (Vara et al. 2004). Gefitinib blocks the PI3K/AKT signaling pathway by competitively binding to the EGFR tyrosine kinase domain (Le et al. 2005). In this study, we showed that PI3K/AKT signaling was inhibited in gefitinib-resistant cells after infection with shGLRX-1 or -2. Moreover, the upregulation of FoxM1 induced by EGFR overexpression was reversed upon treatment with LY294002 and wortmannin. These findings suggest that GLRX may regulate gefitinib resistance via the EGFR/PI3K/AKT/FoxM1 signaling pathway.

Oxidative stress plays a critical role in drug resistance, and increasing levels of ROS which can selectively induce apoptosis in drug-resistant tumor cells (Wang et al. 2018). Consistent with these findings, we showed that knockdown of GLRX significantly increased ROS levels and apoptosis in PC9R cells. Furthermore, we found GLRX was regulated by NRF2, which plays an important role in mediating oxidative stress (Chan et al. 2001; Ma 2013) in PC9R cells. FoxM1 is also an important regulator of oxidative stress (Park et al. 2009). In gefitinib-resistant PC9R cells, FoxM1 silencing dramatically induced ROS generation and cell apoptosis, indicating that GLRX may modulate ROS levels via the FoxM1 signaling pathway.

In summary, our results showed that GLRX expression increases the resistance of NSCLC cells to gefitinib, perhaps through the EGFR/PI3K/AKT/ERK/FoxM1 signaling pathway. This indicates that the targeting of GLRX could be used to sensitize NSCLC cells to gefitinib. GLRX-targeted therapy may therefore be an attractive strategy for use in combination with gefitinib.

Author contributions Jian Zhou, Chunxue Bai, and Yuanlin Song conceived and designed the study. Linlin Wang, Jing Liu, Jinguo Liu, Xiaoyan Chen, Meijia Chang, and Jing Li performed the experiments and statistical analyses. Linlin Wang, Jing Liu, Jinguo Liu, and Xiaoyan Chen wrote the paper. All authors read and approved the final manuscript.

Funding This work was supported by National Science & Technology Major Project "Key New Drug Creation and Manufacturing Program" (no. 2018ZX09201002-006), Natural Science Foundation of China (no. 81570028, 81770039, and 81400018), Zhongshan Hospital Clinical Research Foundation (no. 2016ZSLC05), National Key Technology Research and Development Program of the Ministry of Science and Technology of China (2013BAI09B00), the State Key Basic Research Program (973) project (2015CB553404), and Project of Natural Science Foundation of Shandong Province (ZR2016HL39).

Data Availability The datasets used and/or analyzed during the current study are available from the corresponding author on reasonable request.

Compliance with ethical standards

Conflict of interest Authors have no financial, professional, or personal conflicts to disclose.

Ethical approval Animal experiments were approved by the Research Ethics Committee of Zhongshan Hospital, Fudan University (Shanghai, China) and all applicable international, national, and/or institutional guidelines for the care and use of animals were followed.

Informed consent No human participants were used in this study.

References

Boddupalli S, Mein JR, Lakkanna S, James DR (2012) Induction of phase 2 antioxidant enzymes by broccoli sulforaphane: perspectives in maintaining the antioxidant activity of vitamins a. C e Front Gene 3:7–7. https://doi.org/10.3389/fgene.2012.00007

Chan K, Han X-D, Kan YW (2001) An important function of Nrf2 in combating oxidative stress: detoxification of acetaminophen Proceedings of the National Academy of Sciences 98:4611–4616

Chen G, Kronenberger P, Teugels E, Umelo IA, De Grève J (2012) Targeting the epidermal growth factor receptor in non-small cell lung cancer cells: the effect of combining RNA interference with tyrosine kinase inhibitors or cetuximab. BMC Med 10:28

Elzagallaai A, Garcia-Bournissen F, Finkelstein Y, Bend J, Rieder M, Koren G (2011) Severe bullous hypersensitivity reactions after exposure to carbamazepine in a Han-Chinese child with a positive HLA-B* 1502 and negative in vitro toxicity assays: evidence for different pathophysiological mechanisms. J Popul Ther Clin Pharmacol 18:e1–e9

Ercan D et al (2012) Reactivation of ERK signaling causes resistance to EGFR kinase inhibitors. Cancer Discov https://doi.org/10.1158/2159-8290.cd-12-0103

Ewald JA, Wilkinson JC, Guyer CA, Staros JV (2003) Ligand-and kinase activity-independent cell survival mediated by the epidermal growth factor receptor expressed in 32D cells. Exp Cell Res 282:121–131

Feng F et al (2007) Role of epidermal growth factor receptor degradation in gemcitabine-mediated. Cytotox Oncogene 26:3431

Gallogly MM, Starke DW, Mieyal JJ (2009) Mechanistic and kinetic details of catalysis of thiol-disulfide exchange by glutaredoxins and potential mechanisms of regulation. Antioxid Redox Signal 11:1059–1081. https://doi.org/10.1089/ars.2008.2291

Gallogly MM et al (2010) Glutaredoxin regulates apoptosis in cardiomyocytes via NFκB targets Bcl-2 and Bcl-xL. Implic Cardiac Aging Antioxid Redox Signal 12:1339–1353. https://doi.org/10.1089/ars.2009.2791

Gladyshev VN et al (2001) Identification and characterization of a new mammalian glutaredoxin (thioltransferase), Grx2. J Biol Chem 276:30374–30380

Holmgren A (1976) Hydrogen donor system for Escherichia coli ribonucleoside-diphosphate reductase dependent upon glutathione. Proc Natl Acad Sci USA 73:2275–2279

Holmgren A (1979) Glutathione-dependent synthesis of deoxyribonucleotides. Purification and characterization of glutaredoxin from *Escherichia coli*. J Biol Chem 254:3664–3671

Kris MA (2002) Phase II trial of ZD1839 (" Iressa") in advanced non-small-cell lung cancer (NSCLC) patients who had failed platinum- and docetaxel-based regimens (IDEAL 2). In: Proc Am Soc Clin Oncol, p 292a

Le X-F, Pruefer F, Bast RC (2005) HER2-targeting antibodies modulate the cyclin-dependent kinase inhibitor p27Kip1 via multiple signaling pathways. Cell Cycle 4:87–95

Liu X, Jann J, Xavier C, Wu H (2015) Glutaredoxin 1 (Grx1) protects human retinal pigment epithelial cells from oxidative damage by preventing AKT glutathionylation invest. Ophthalmol Vis Sci 56:2821–2832. https://doi.org/10.1167/iovs.14-15876

Lundberg M et al (2001) Cloning and expression of a novel human glutaredoxin (Grx2) with mitochondrial and nuclear isoforms. J Biol Chem 276:26269–26275

Ma Q (2013) Role of nrf2 in oxidative stress and toxicity. Ann Rev Pharmacol Toxicol 53:401–426

Mollbrink A et al (2014) Expression of thioredoxins and glutaredoxins in human hepatocellular carcinoma: correlation to cell proliferation, tumor size and metabolic syndrome. Int J Immunopathol Pharmacol 27:169–183

Nagy P, Arndt-Jovin DJ, Jovin TM (2003) Small interfering RNAs suppress the expression of endogenous and GFP-fused epidermal growth factor receptor (erbB1) and induce apoptosis in erbB1-overexpressing cells. Exp Cell Res 285:39–49

Nelson MH, Dolder CR (2006) Lapatinib: a novel dual tyrosine kinase inhibitor with activity in solid tumors. Ann Pharmacother 40:261–269. https://doi.org/10.1345/aph.1G387

Nicholson R, Gee J, Harper M (2001) EGFR and cancer prognosis. Eur J Cancer 37:9–15

Pao W, Chmielecki J (2010) Rational, biologically based treatment of EGFR-mutant non-small-cell lung cancer. Nat Rev Cancer 10:760–774. https://doi.org/10.1038/nrc2947

Park HJ et al (2009) FoxM1, a critical regulator of oxidative stress during oncogenesis. EMBO J 28:2908–2918. https://doi.org/10.1038/emboj.2009.239

Raychaudhuri P, Park HJ (2011) FoxM1: a master regulator of tumor metastasis. Cancer Res 71:4329–4333

Rho JK et al (2009) The role of MET activation in determining the sensitivity to epidermal growth factor receptor tyrosine kinase inhibitors. Mol Cancer Res 7:1736–1743. https://doi.org/10.1158/1541-7786.MCR-08-0504

Rodriguez-Rocha H, Garcia Garcia A, Zavala-Flores L, Li S, Madayiputhiya N, Franco R (2012) Glutaredoxin 1 protects dopaminergic cells by increased protein glutathionylation in experimental Parkinson's disease. Antioxid Redox Signal 17:1676–1693. https://doi.org/10.1089/ars.2011.4474

Sun H et al (2011) FOXM1 expression predicts the prognosis in hepatocellular carcinoma patients after orthotopic liver transplantation combined with the Milan criteria. Cancer Lett 306:214–222

Tan X, Thapa N, Sun Y, Anderson RA (2015) A kinase-independent role for EGF receptor in autophagy. Initiat Cell 160:145–160

Vara JÁF, Casado E, de Castro J, Cejas P, Belda-Iniesta C, González-Barón M (2004) PI3K/Akt signalling pathway and cancer. Cancer Treat Rev 30:193–204

Wakeling AE, Guy SP, Woodburn JR, Ashton SE, Curry BJ, Barker AJ, Gibson KH (2002) ZD1839 (Iressa): an orally active inhibitor of epidermal growth factor signaling with potential for cancer therapy. Cancer Res 62:5749–5754

Wang L et al (2018) An acquired vulnerability of drug-resistant melanoma with therapeutic potential cell https://doi.org/10.1016/j.cell.2018.04.012

Weihua Z, Tsan R, Huang W-C, Wu Q, Chiu C-H, Fidler IJ, Hung M-C (2008) Survival of cancer cells is maintained by EGFR independent of its kinase activity. Cancer Cell 13:385–393

Xu N et al (2012) FoxM1 mediated resistance to gefitinib in non-small-cell lung cancer cells. Acta Pharmacol Sin 33:675

Yamanaka S et al (2008) siRNA targeting against EGFR, a promising candidate for a novel therapeutic application to lung adenocarcinoma. Pathobiology 75:2–8

Yang F, Yi M, Liu Y, Wang Q, Hu Y, Deng H (2018) Glutaredoxin-1 silencing induces cell senescence via p53/p21/p16 signaling axis. J Proteome Res 17:1091–1100. https://doi.org/10.1021/acs.jproteome.7b00761

Yewale C, Baradia D, Vhora I, Patil S, Misra A (2013) Epidermal growth factor receptor targeting in cancer: a review of trends and strategies. Biomaterials 34:8690–8707. https://doi.org/10.1016/j.biomaterials.2013.07.100

Yu J et al (2011) Array-based comparative genomic hybridization identifies CDK4 and FOXM1 alterations as independent predictors of survival in malignant peripheral nerve sheath tumor. Clin Cancer Res 17:1924–1934

Zhang F et al (2018) FOXK2 suppresses the malignant phenotype and induces apoptosis through inhibition of EGFR in clear-cell renal cell carcinoma. Int J Cancer. https://doi.org/10.1002/ijc.31278